Loss of RdDM-independent CHH methylation is sufficient for disruption of chromosome-specific rRNA gene silencing

Anastasia McKinlay[1,†], Ramya Enganti[1,†], Navinchandra V. Puppala[2,†], Gargi P. Saradadevi[2,†], Todd Blevins[3] , and Gireesha Mohannath[2*]

[1]Department of Biology and Department of Molecular and Cellular Biochemistry, Indiana University, Bloomington, IN, United States.

[2]Department of Biological Sciences, Birla Institute of Technology and Science-Pilani, Hyderabad campus, Hyderabad, Telangana, India.

[3]Institut de Biologie Moléculaire des Plantes, CNRS, Université de Strasbourg, Strasbourg, France.

† These authors contributed equally to this work

Corresponding author:
Email: gireesha@hyderabad.bits-pilani.ac.in

Summary

Arabidopsis thaliana has two nucleolus organizer regions (NORs), consisting of long tandem arrays of 45S rRNA genes on chromosomes 2 (NOR2) and 4 (NOR4). The rRNA gene subtypes mapping to NOR2 are mostly silenced during development, whereas those mapping to NOR4 are active. By analyzing DNA methylation-deficient Arabidopsis mutants, we found that the degree of disruption of NOR2 rRNA gene silencing correlates consistently with the loss of rDNA cytosine methylation in the CHH sequence context, rather than with

methylation losses in CG or CHG contexts. Comparison of Arabidopsis and tomato NOR sequences revealed that rRNA gene promoter cytosines mostly occur in the CHH context, followed by fewer sites in the CHG context. By contrast, almost no CG dinucleotides occur in plant rRNA gene promoters. This prevalence of CHH sites in plant rDNA promoters suggests a mechanism to explain the stronger disruption of NOR2 gene silencing in CHH methylation mutants lacking CHROMOMETHYLASE 2 (CMT2) or DECREASE IN DNA METHYLATION 1 (DDM1) functions as compared to other DNA methylation-deficient mutant lines. Notably, CMT2 mediates CHH methylation independently of RNA-directed DNA methylation factors but with a requirement for the chromatin remodeler DDM1. Furthermore, we demonstrate that NOR2 genes are hypermethylated and exist in more condensed chromatin than NOR4 genes. Collectively, our data define a critical role for CHH methylation in plant rRNA gene silencing, which is mostly mediated by CG methylation in mammals.

Key words:
Ribosomal RNA (rRNA), rDNA promoter, Nucleolus organizer region (NOR), Gene silencing, DNA cytosine methylation, chromatin

Significance Statement

In plants, DNA cytosine methylation occurs in three sequence contexts (CG, CHG, and CHH), but it was not clear how these distinct contexts contribute to chromosome-specific large-scale rRNA gene silencing. Using rRNA gene expression, methylation assays, and bioinformatic analysis of rDNA promoters and methylation patterns, this study shows that CHH methylation, rather than CG or CHG methylation, plays a critical role in plant rRNA gene silencing, which is mostly mediated by CG methylation in mammals.

Introduction

In eukaryotes, hundreds to thousands of 45S ribosomal RNA (rRNA) genes are arranged as tandem repeats at chromosomal loci known as nucleolus organizer regions (NORs) (Gerbi, 1986, Long and Dawid, 1980, Viktorovskaya and Schneider, 2015). RNA polymerase I (Pol I) transcribes rRNA genes to produce 45S pre-rRNA transcripts that are then processed into 18S, 5.8S, and 25-28S rRNAs that comprise the catalytic core of ribosomes, which

synthesize proteins in cells (Saradadevi et al., 2020, Turowski and Tollervey, 2015, Viktorovskaya and Schneider, 2015). Although eukaryotic genomes have many rRNA genes, not all of them are transcribed all the time. Rather, the number of genes transcribed varies during development, dictated by the developmental stage-specific need for ribosomes and protein synthesis (Grummt, 2013, Hannan et al., 2013, Moss et al., 2007). rRNA 'dosage control' involves selective gene silencing rather than selective gene activation (Chen and Pikaard, 1997, Pikaard et al., 2023). In *Arabidopsis thaliana*, rRNA genes are clustered within two NORs located at the northern tips of chromosomes 2 (*NOR2,* which spans ~ 5.9 Mb) and 4 (*NOR4,* which spans ~ 3.9 Mb) (Copenhaver et al., 1995, Copenhaver and Pikaard, 1996b, Copenhaver and Pikaard, 1996a, Fultz et al., 2023). Recent findings in *A. thaliana* demonstrated that the selective rRNA gene silencing is determined by their chromosomal location, not rRNA gene sequence variation (Chandrasekhara et al., 2016, Mohannath et al., 2016). During development, rRNA genes located on *NOR2* are selectively silenced while those on *NOR4* remain active (Chandrasekhara et al., 2016, Mohannath et al., 2016).

Transcriptional gene silencing in eukaryotes often involves cytosine methylation and chromatin condensation (Rhee et al., 2002, Zhang et al., 2006, Zilberman et al., 2007). However, the relative role of cytosine methylation in all three sequence contexts (CG, CHG, and CHH, where H=A, C, or T) in selectively silencing *NOR2* rRNA genes is unknown. In plants, cytosine methylation is deposited by several DNA methyltransferases belonging to different families. METHYLTRANSFERASE 1 (MET1) and CHROMOMETHYLASE 3 (CMT3) mediate virtually all Arabidopsis CG and CHG methylation, respectively (Cokus et al., 2008, Lister et al., 2008, Zemach et al., 2013). CHH methylation is directed by small RNAs and mediated by DOMAINS REARRANGED METHYLTRANSFERASE 2 (DRM2) via the RNA-directed DNA methylation (RdDM) pathway, but also by CHROMOMETHYLASE 2 (CMT2) independently of RdDM (Zemach et al., 2013, Law and Jacobsen, 2010, Rymen et al., 2020, Sasaki et al., 2019). *CMT2* and *CMT3* belong to a group of plant-specific chromomethylases (Bewick et al., 2017). *cmt2-3* mutation is known to reduce most of the CHH methylation (Zemach et al., 2013). In addition to the abovementioned DNA methyltransferases, DECREASE IN DNA METHYLATION 1 (*DDM1*), a SWI2/SNF2 family chromatin remodeler, acts as a master regulator of DNA methylation (Brzeski and Jerzmanowski, 2003, Lee et al., 2023, Osakabe et al., 2021). Loss of DDM1 results in genome-wide demethylation at 70% of methylated cytosines in all three sequence contexts (CG, CHG, and CHH) (Jeddeloh et al., 1999, Vongs et al., 1993, Zemach et al., 2013).

An earlier study investigated the effects of *drm2*, *cmt3,* and *met1* mutants on rRNA gene silencing (Pontvianne et al., 2013). These mutants predominantly show loss of CG or

107 CHG methylation with minimal to modest loss of CHH methylation (Cokus et al., 2008,
108 Zemach et al., 2013). In this study, we analysed *ddm1* and *cmt2* mutants, which display
109 significant losses in CHH methylation when compared to *drm2*, *cmt3*, and *met1* mutants. We
110 studied these five DNA methylation-deficient mutants to compare the relative effects of
111 differential loss of CG, CHG, and CHH methylation on the disruption of chromosome-specific
112 *NOR2* rRNA gene silencing. In this mutant panel, we show a correlation between the relative
113 loss in *NOR2* rRNA gene silencing and the disruption of cytosine methylation at CHH sites,
114 but not at CG or CHG sites within rDNA loci.
115 By analyzing the 45S rRNA gene promoters using the recently assembled and
116 published NOR sequences of Arabidopsis (a total of ~950 45S rRNA genes) (Fultz et al.,
117 2023) and tomato (a total of ~1500 45S rRNA genes) (Shirasawa and Ariizumi, 2023), we
118 found that 45S rRNA gene promoter cytosines are mostly in the CHH context, distantly
119 followed by the CHG context and with almost no cytosines in the CG context, providing a
120 putative mechanistic basis for higher *NOR2* derepression observed in *cmt2* and *ddm1*
121 mutants that display higher losses of CHH methylation than other mutants. Lastly, using
122 multiple methylation and chromatin condensation assays, we show that *NOR2* rRNA genes
123 are hypermethylated and exist in more condensed chromatin than *NOR4* genes. In contrast
124 to the key role of CG methylation in mammalian rRNA gene regulation, our study
125 demonstrates a critical role for CHH methylation mediated by CMT2 in plant rRNA gene
126 regulation.
127
128 **Results**
129 **Selective *NOR2* rRNA gene silencing is disrupted in DNA methylation mutants**
130 The rRNA genes in *A. thaliana* are organized into two tandem arrays on NORs, one each on
131 chromosomes 2 (*NOR2*), and 4 (*NOR4*) (Figure 1). In the reference strain Col-0, *NOR2* is
132 5.5 Mb and *NOR4* is 3.9 Mb, with ~550 and ~390 tandem repeats of 45S rRNA genes,
133 respectively (Fultz et al., 2023) (Figure 1). The 18S, 5.8S, and 25S rRNA sequences are
134 identical among 45S rRNA genes, but variation exists in the internal transcribed spacer (ITS)
135 and the external transcribed spacer (ETS) regions. Four distinct variants, named VAR1
136 through VAR4 had previously been defined based on the length polymorphism in the 3' ETS
137 region (Pontvianne et al., 2010) (Figure 1B-C). Of these, VAR1, VAR2, and a subset of
138 VAR3 (VAR3a) lack HindIII sites in the 3' ETS region, but the remaining variants (VAR3b,c
139 and VAR4) have a HindIII site (Chandrasekhara et al., 2016, Mohannath et al., 2016)
140 (Fig.1C). During development, the rRNA gene variants that map primarily to *NOR2* (VAR1,
141 VAR3a) are selectively silenced as a consequence of dosage control. In contrast, the

142 variants that map primarily to *NOR4* (VAR2, VAR3c, and VAR4) remain active (Figure
143 1D)(Chandrasekhara et al., 2016).

144 To determine the relative impact of loss of CG, CHG, and CHH methylation on
145 selective *NOR2* rRNA gene silencing, we analysed rRNA variant expression in the mutants
146 defective for DNA methylation, which include *ddm1*, *cmt2*, *met1*, *cmt3*, and *drm2* mutants. In
147 these mutants and the WT-Col-0 strain, we performed RT-PCR analysis using RNA isolated
148 from 4-week-old leaf tissues. VAR1 type rRNA genes constitute ~50% of total 45S rRNA
149 genes, and most of them map to *NOR2*, and undergo selective silencing during development
150 (Chandrasekhara et al., 2016, Pontvianne et al., 2010). Our results showed that among the
151 DNA methylation mutants, VAR1 expression levels were found to be the highest in *cmt2 and*
152 *ddm1,* followed by *met1* mutants (Figure 2). In contrast, the *cmt3* and *drm2* mutants have
153 displayed low levels of VAR1 expression, close to that of wild-type Col-0 plants (Figure 2).

154 Using published whole-genome bisulfite sequencing data (Stroud et al., 2013), we
155 generated heatmaps of cytosine methylation for a 45S rRNA reference gene sequence
156 (Figure S2) using Methylpy (Schultz et al., 2015) (Figure 3). The rDNA cytosine methylation
157 heatmaps show the highest loss of CHH methylation in *cmt2*, followed by *ddm1* mutants
158 (Figure 3). Indeed these mutants also show higher *NOR2* gene silencing disruption than the
159 other mutants (Figure 2). Next, *met1* mutants showed loss of CHH methylation and *NOR2*
160 gene silencing disruption, which in degree are lower compared to *cmt2* and *ddm1* mutants
161 (Figs 2 &3). Lastly, among all, *cmt3* and *drm1drm2* mutants showed the least CHH
162 methylation loss at rDNA loci (Figure 3) and the least *NOR2* gene silencing disruption
163 (Figure 2). Interestingly, the minimal loss of rDNA CHH methylation in *drm1drm2,* known
164 RdDM mutants, indicate that CHH methylation at rDNA loci is mostly mediated by RdDM-
165 independent *CMT2*, providing one more basis for the highest *NOR2* gene silencing
166 disruption observed in *cmt2* mutants (Figs. 2&3).

167 Next, the highest loss of CG methylation at rDNA loci was found in *ddm1* and *met1*
168 mutants and the highest loss of CHG methylation was found in *ddm1* and *cmt3* mutants
169 (Figure 3). Based on the data from Figures 2 and 3, we conclude that the degree of
170 disruption of *NOR2* rRNA gene silencing consistently correlates with the levels of CHH
171 methylation loss, rather than the levels of CG or CHG methylation loss, at rDNA loci. Our
172 data depicting varying loss of CG, CHG, and CHH methylation at rDNA loci in *met1*, *cmt3*,
173 and *drm2* mutants are consistent with findings from a previous study (Cokus et al., 2008).
174 However, *ddm1* and *cmt2* mutants were not previously analyzed for context-specific cytosine
175 methylation loss at rDNA loci or for their effects on disruption of selective *NOR2* rRNA gene
176 silencing. Studying these mutants turned out to be key in establishing a critical role for CHH
177 methylation in the selective *NOR2* rRNA gene silencing.

178 Next, we wondered why when compared to CHH methylation loss, CG or CHG
179 methylation loss does not significantly impact *NOR2* rRNA gene silencing despite the *NOR2*
180 genes showing the highest levels of CG methylation, followed by CHG methylation (Fultz et
181 al., 2023, Mo et al., 2023). To address this question, we first analyzed the distribution of
182 cytosines in CG, CHG, and CHH sequence contexts in the rRNA gene promoter regions of
183 the recently assembled and published NOR sequences in *A. thaliana* (Col-0 strain),
184 constituting a total of ~ 950 copies of 45S rRNA genes (Doelling and Pikaard, 1995, Fultz et
185 al., 2023). In Arabidopsis, -55 to +6 region with respect to the transcription start site (+1) in
186 the 45S rRNA genes constitutes the gene promoter region (Doelling et al., 1993, Doelling
187 and Pikaard, 1995). () First, we found that the gene promoter has eight cytosines but
188 strikingly, none of them exist in CG context. Six (75%) exist in CHH context and the
189 remaining two (25%) exist in CHG context (Figure 4). Next, we found that the gene promoter
190 region is highly conserved across most of the *A. thaliana* 45S rRNA genes (Fultz et al.,
191 2023). Of 894 total 45S rRNA gene repeats combinedly present on *NOR2* and *NOR4*, 859
192 repeats (96%) showed 100% homology to the gene promoter sequence (-55 to +6) (Figure
193 4B, 5th column). The remaining repeats showed one to few mismatches. Further, we
194 extended our analysis to -300 bp to include the upstream promoter region (Pontvianne et al.,
195 2013), which had showed only a small positive effect on transcription of 45S rRNA genes
196 (Doelling et al., 1993, Doelling and Pikaard, 1995), and these upstream sequences are not
197 conserved among 45S rRNA genes (Fultz et al., 2023). Among the 51 cytosines found in this
198 region, again, predominant occurrence of cytosines was found in the CHH context (41
199 cytosines; ~80%), distantly followed by the CHG (6 cytosines; ~12%) and the CG (4
200 cytosines; ~8%) contexts (Figure S3-A).
201 Similarly, we analysed gene promoter regions in the recently assembled tomato
202 *NOR2* constituting ~1500 45S rRNA genes (Shirasawa and Ariizumi, 2023) and the
203 previously published tomato 45S rRNA gene promoter sequence (Doelling and Pikaard,
204 1995). First, we found that the gene promoter has 12 cytosines, of which 10 (~83%) exist in
205 the CHH context, 2 (~17%) the CHG context, and none in the CG context (Figure 4)
206 (Doelling and Pikaard, 1995, Shirasawa and Ariizumi, 2023). We also found the gene
207 promoter sequences to be highly conserved across the tomato *NOR2*. Of 1500 total 45S
208 rRNA gene repeats present on *NOR*2, 1473 repeats (98%) showed 100% homology to the
209 gene promoter sequence (-55 to +6) (Figure 4B, 5th column) (Shirasawa and Ariizumi, 2023)
210 and the remaining repeats showed one to few mismatches. The results also appear to be
211 similar in other plant species (Figure 4) (Doelling and Pikaard, 1995). Collectively, the rDNA
212 promoter analyses across different plant species provide a putative mechanistic basis for
213 maximum disruption of *NOR2* rRNA gene silencing observed in the *cmt2* and *ddm1* mutants

214 that displayed the highest loss of CHH methylation. Overall, these results define a novel
215 critical role for CHH methylation in 45S rRNA gene regulation in plants.
216 In contrast, when we analyzed known human rDNA promoter sequences (Zhou et al.,
217 2016), we found that out of 65 cytosines, 26 are in CG (~40%; the highest among the three),
218 19 in CHG (~29%), and 20 in CHH (~31%) contexts (Figure S3.B). These results are
219 consistent with the mammalian rRNA gene regulation, which is almost entirely dictated by
220 CG methylation (Bernstein et al., 2007, Priyadarshini et al., 2023, Zhou et al., 2016). These
221 results indicate the presence of evolutionarily divergent mechanisms of rRNA gene
222 regulation between plants and mammals.
223

224 ***NOR2* rRNA genes are hypermethylated while *NOR4* rRNA genes are hypomethylated**
225 **in Col-0**

226 We carried out methylation analysis of rRNA variants using HpaII-digested genomic DNA
227 (gDNA) of Col-0 and *met1* mutants (Figure 5). Because the rRNA variant-defining 3' ETS
228 region lacks HpaII sites, HpaII digestion of gDNA does not impact PCR amplification of this
229 region. Therefore, we chose to separate HpaII-digested and HpaII-undigested fractions of
230 gDNA by resolving them on an agarose gel. The fragments that remained at the top of the
231 gel (>20 kb) constituted the HpaII-undigested fractions while those resolved at 0.6-1.0 kb
232 range constituted the HpaII-digested fractions (Figure 5A, left panel). Both the digested and
233 the undigested fractions were gel-eluted, followed by PCR amplification of rRNA variants.
234 Through this analysis, we were able to identify the rRNA variants that were enriched in
235 HpaII-digested or undigested fractions. The PCR data revealed VAR2 genes from *NOR4* to
236 be the most predominant in Col-0 among the HpaII-digested products, indicating relative
237 hypomethylation of *NOR4* genes compared to *NOR2*-localized VAR1 genes (Figure 5A,
238 lanes 1 and 2, right panel). However, in *met1* mutants, used as a control, all rRNA variants
239 were amplified proportionate to their composition due to loss of cytosine methylation in all of
240 them (Figure 5A, lanes 3 and 4, right panel,).
241 In another experiment, we subjected gDNA to digestion by McrBC, an enzyme that
242 preferentially digests DNA if its recognition site ($R^mC(N_{40\text{-}3000})R^mC$) consists of methylated
243 cytosines. McrBC digestion of gDNA followed by PCR amplification of rRNA variants
244 revealed that VAR1 was digested the most and VAR2 the least (Figure 5B), indicating that
245 *NOR2* genes are hypermethylated in contrast to *NOR4* genes, consistent with recent
246 findings in Arabidopsis which employed sequencing-based methylation analysis of rRNA
247 variants (Fultz et al., 2023, Mo et al., 2023).
248

249 ***NOR2* rRNA genes are hypermethylated while *NOR4* rRNA genes are hypomethylated**
250 **in the introgression line Col$^{Sf\text{-}NOR4}$**
251 In a previous study, we showed that an introgression line named Col$^{Sf\text{-}NOR4}$ consists of *NOR2*
252 from Col-0 (VAR1 and VAR3 genes) and *NOR4* from Sf-2 ecotype (Chandrasekhara et al.,
253 2016) (Figure 6A). Sf-2 has only VAR1 type of rRNA genes, but they can be differentiated
254 from VAR1 genes of Col-0 by HindIII digestion. Sf-2 VAR1 genes have a HindIII site in their
255 3' ETS region, while Col-0 VAR1 genes lack it (Chandrasekhara et al., 2016). In Col$^{Sf\text{-}NOR4}$,
256 Sf-2 *NOR4* genes are active though they are similar in sequence to the silenced Col-0 *NOR2*
257 (VAR1) genes (Chandrasekhara et al., 2016). However, Col-0 *NOR2* genes are still
258 selectively silenced in Col$^{Sf\text{-}NOR4}$ (Chandrasekhara et al., 2016). Therefore, we analyzed this
259 introgression line to see if VAR1 type of genes residing in *NOR2* and *NOR4* of Col$^{Sf\text{-}NOR4}$ are
260 differentially methylated or not, using similar methylation assays, as described above. In one
261 experiment, gDNA of Col$^{Sf\text{-}NOR4}$ was subjected to HpaII digestion, followed by gel elutions of
262 the undigested and the digested fractions. The gel-eluted DNA samples were then subjected
263 to PCR amplification of rRNA variants followed by HindIII digestion. In control samples (no
264 HpaII), HindIII digestion of PCR-amplified rRNA variants resulted in the expected products,
265 which include digested Sf2-VAR1 genes, undigested Col-0 VAR1 genes, and partially
266 digested Col-0 VAR3 genes (Figure 6B, lanes 1 and 2, top right gel image, and Figure 6C)
267 (Chandrasekhara et al., 2016). However, HindIII digestion of the PCR products obtained
268 from the gel-purified HpaII-digested fraction as the template, revealed that Col-0 VAR1
269 genes predominantly constitute the HpaII-undigested fraction (Figure 6B, lanes 3 and 4, top
270 right gel image, and Figure 6C). On the other hand, we observed a significant increase in the
271 Sf-2 VAR1 genes in the HpaII-digested fraction (Figure 6B, lanes 3 and 4, bottom right gel
272 image, and Figure 6C) compared to the undigested fraction (Figure 6B, lanes 3 and 4, top
273 right gel image, and Figure 6C). These data indicate hypermethylation of Col-0 *NOR2* genes
274 and hypomethylation of Sf-2 *NOR4* genes, despite the presence of the VAR1 type of genes
275 on both the NORs in the Col$^{Sf\text{-}NOR4}$ introgression line.
276 In another experiment, gDNA of Col$^{Sf\text{-}NOR4}$ was first digested with McrBC, followed by
277 PCR amplification of rRNA variants. These PCR products were then digested with HindIII
278 and resolved using regular gel electrophoresis. HindIII-digested control PCR products (no
279 McrBC digestion) behaved as expected based on the presence or the absence of HindIII
280 sites (Figure 6D, E, lanes 1 and 2). However, the McrBC digestion patterns of the rRNA
281 variants (Figure 6D, E) were the opposite of the experimental results involving HpaII
282 digestion (compare to Figure 6B, C). Predominantly, the Sf-2 VAR1 genes constituted the
283 McrBC-undigested fraction, while the Col-0 VAR1 genes constituted the McrBC-digested
284 fraction (Figure 6D, E, lanes 3 and 4). We also observed complete digestion of the Col-0

285 VAR3 (from *NOR2*) genes by McrBC (Figure 6D, lane 3). These data again demonstrate that
286 *NOR4* genes are hypomethylated and *NOR2* genes are hypermethylated in $Col^{Sf\text{-}NOR4}$.
287 In Figures 4 and 5, resistance to HpaII digestion indicates the presence of CG and
288 CHG methylation while digestion by McrBC indicates the prevalence of CG, CHG, and CHH
289 methylation. Based on these data we conclude that *NOR2* genes are hypermethylated than
290 *NOR4* genes, in all cytosine contexts.
291
292 ***NOR2* rRNA genes exist in more condensed chromatin than *NOR4* rRNA genes**
293 To investigate the chromatin accessibility of *NOR2* and *NOR4* genes, we carried out Tn5
294 transposase-mediated transposition using nuclei isolated from 3-week-old Col-0 plants. Tn5
295 is a prokaryotic hyperactive transposase that has been developed as a tool to insert short
296 DNA sequences into open chromatin regions (Adey et al., 2010, Goryshin and Reznikoff,
297 1998, Buenrostro et al., 2013). A pair of 19 bp IS50 repeats that serve as 'outside ends'
298 (OEs) sequences are sufficient for recognition by Tn5 transposase and transposition of OEs-
299 containing sequences into open chromatin (Ahmed, 2009). We designed short DNA
300 sequences consisting of OEs for Tn5 recognition and used them in a native chromatin
301 transposition assay. Purified Col-0 nuclei were incubated with or without 5 pmol oligos
302 containing Tn5 recognition sites for transposition, followed by DNA extraction from the nuclei
303 and PCR analysis of rRNA variants. The PCR data did not reveal differences between *NOR2*
304 and *NOR4* genes. We then tried an indirect approach to focus on the chromatin accessibility
305 state of the promoter regions. In this approach, the DNA samples isolated from Tn5
306 transposase-treated nuclei were subjected to two rounds of PCR amplification. The first
307 round of PCR (PCR1) amplifies ~2.8 kb region that spans the 3' ETS region, IGS, and the
308 promoter of the following 45S rRNA gene repeat (Figure 7 A-B). Due to the lack of variant-
309 specific sequence variation in the promoter region, we exploited the proximity of the rRNA
310 variant-defining 3' ETS region of one rRNA gene to the promoter of the following rRNA gene.
311 The occurrence of rRNA genes as tandem repeats (Figure 1A) at NORs permitted this
312 approach. The idea is that, if promoters of VAR1 genes (primarily present on *NOR2*) are
313 more condensed than the promoters of VAR2 genes (primarily present on *NOR4*), then the
314 2.8 kb PCR products should be enriched for VAR1 genes. Because the 2.8 kb PCR products
315 obtained during PCR1 (using primers 5'allvar and p34) cannot discriminate between *NOR2*
316 and *NOR4* genes, they were resolved on a 1% agarose gel followed by gel-purification of 2.8
317 kb amplicons. These amplicons were then subjected to the second round of PCR
318 amplification (PCR2) with primers that either amplified only VAR1 and VAR2 genes (Figure
319 7C) or all four rRNA variants (Figure 7D). The results showed severe depletion of *NOR4*-
320 specific VAR2 genes in the reactions with 5 pmol of Tn5 oligos (Figure 7C, D), indicating

321 depletion of *NOR4*-specific fragments in the PCR1 amplicon pool. This depletion is
322 presumably due to higher transposition rates in the promoter regions of *NOR4*-specific rRNA
323 genes compared to the *NOR2* genes. Collectively, these data indicate that *NOR4* genes are
324 predominantly present in a more accessible open chromatin state than *NOR2* genes,
325 consistent with recent findings from a chromatin condensation study in Arabidopsis (Mo et al.,
326 2023).

327 It is still not clear why *NOR2* rRNA genes selectively undergo hypermethylation and
328 chromatin condensation. Methylation maps of centromere-proximal regions of NORs show
329 that ~ 75 kb of the *NOR2*-adjoining region, composed of transposable elements and
330 transposon remnants, is heavily methylated in all cytosine contexts compared to the *NOR4*-
331 adjoining region (Figure S4), which has a protein-coding gene just 3 kb away (Lewis and
332 Pikaard, 2001) and do not contain any stretch of transposons or their remnants thereafter. In
333 plants, transposons are silenced through DNA methylation-mediated mechanisms. Could
334 such silencing of the *NOR2*-adjoining transposon-rich region spread to *NOR2* rRNA genes,
335 resulting in their selective silencing? The question remains to be answered.

336

337 **Discussion**

338 To know the relative role of cytosine methylation in each sequence context (CG, CHG, and
339 CHH) in *NOR2* rRNA gene silencing, we analyzed various DNA methylation-deficient
340 mutants of Arabidopsis that display loss of CG, CHG, and CHH methylation to varying
341 degrees. In Arabidopsis, CHH methylation is mainly determined by RdDM-dependent DRM2
342 and RdDM-independent CMT2 (Rhee et al., 2002, Stroud et al., 2013, Zemach et al., 2013).
343 Between these two, CMT2 appears to be responsible for most of the CHH methylation at
344 rDNA loci (Figure 3). Interestingly, cytosines in plant rRNA gene promoters, including those
345 of Arabidopsis predominantly occur in the CHH context followed by a few in the CHG context
346 and almost none in the CG context (Figure 4 and Figure S3-A). These data potentially
347 explain why *cmt2* mutants displayed the highest *NOR2* gene silencing disruption, despite
348 showing minimal loss of CG or CHG methylation (Figs. 2&3). Therefore, we propose to rule
349 out a significant role for CG or CHG methylation in rRNA gene silencing.

350 CMT2 and CMT3, methylate DNA through the dual binding of H3K9 di-methylation
351 (H3K9me2)-containing nucleosomes via their bromo adjacent homology (BAH) and Chromo
352 domains (Du et al., 2012). Interestingly, it has been found that H3K9 methyltransferases are
353 required for rRNA variant-specific silencing in *A. thaliana* (Pontvianne et al., 2012).
354 Therefore, it is likely that nucleosomes in *NOR2* rRNA gene promoters undergo H3K9
355 dimethylation followed by CHG and CHH methylation, resulting in heterochromatinization
356 and silencing. However, the loss of CHH methylation at rDNA loci has more impact on *NOR2*

357 derepression than the loss of CHG methylation presumably due to the predominant
358 occurrence of cytosines in the CHH context than the CHG context in the rRNA gene
359 promoters (Figs. 2-4).

360 Next, because DDM1 mediates CHH methylation by CMT2 (Zemach et al., 2013), it
361 is reasonable to find levels of CHH methylation loss and *NOR2* gene silencing in *ddm1*
362 mutants comparable to that of *cmt2* mutants (Figs. 2&3). Recent findings have shown that
363 DDM1 deposits histone variant H2A.W, which marks plant heterochromatin, onto potentially
364 mobile transposable elements (TEs) resulting in their transcriptional gene silencing
365 (Osakabe et al., 2021). It remains to be determined if a similar mechanism involving DDM1-
366 mediated histone H2A.W deposition is involved in *NOR2* rRNA gene silencing.

367 Due to apparent lack of a significant role of CG or CHG methylation in rRNA gene
368 silencing (Figs. 2&3), we surmise that the *NOR2* gene silencing disruption observed in *ddm1*
369 and *met1* mutants (Figure 2) is primarily due to their loss of CHH methylation at rDNA loci
370 than due to their loss of CG or CHG methylation (Figure 3). Overall, the data establish a
371 novel critical role for CMT2-mediated RdDM-independent CHH methylation in plant rRNA
372 gene regulation, as shown in our proposed model in Figure 8.

373 It is interesting to note that knocking down DNA methyltransferases MET1 or CMT3,
374 responsible for maintaining methylation in CG and CHG contexts respectively, did not affect
375 nucleolar dominance in tetraploid species *Arabidopsis suecica,* in which rRNA genes from
376 one of the progenitor species *A. thaliana* are silenced during development, while those from
377 the other progenitor species *A. arenosa* remain active (Costa-Nunes et al., 2010). In contrast,
378 knocking down DRM2 DNA methyltransferase (responsible for most of the RdDM-dependent
379 CHH methylation) disrupted nucleolar dominance via release of silencing of *A. thaliana* rRNA
380 genes (Costa-Nunes et al., 2010). Therefore, we predict that the loss of CMT2, responsible
381 for most of the RdDM-independent CHH methylation, would severely impact nucleolar
382 dominance in *A. suecica*, but this prediction needs to be tested.

383 In a similar study in plant species *Tragopogon porrifolius*, the methylation dynamics
384 of cytosines in CWG sequence contexts (where W= A or T) has been suggested to be most
385 responsible for regulating silent and active rDNA states (Matyášek et al., 2024). It would be
386 interesting to know if similar conservation and enrichment of cytosines in the CWG context
387 among the rDNA gene promoters exist in *Tragopogon porrifolius*. Such a cytosine
388 enrichment would indicate the possibility of involvement of different plant-specific
389 chromomethyltransferases (CMTs) in different plant species. Nevertheless, several findings
390 in multiple plant species collectively underscore the importance of non-CG methylation in
391 plant rRNA gene silencing.

392 In contrast to plant species, CG methylation is known to play a prominent role in
393 mammalian rRNA gene regulation. For example, human rDNA promoters are mostly
394 methylated in the CG context and their dysregulation has been linked to several types of
395 cancers (Priyadarshini et al., 2023, Bacalini et al., 2014, Ghoshal et al., 2004, Karahan et al.,
396 2015, Raval et al., 2012, Zhou et al., 2016). Moreover, cytosines occur predominantly in the
397 CG context in the human rRNA gene promoters (Figure S3-B). CHG and CHH methylation
398 are largely absent in mammals, but they occur commonly in plant genomes, carried out
399 predominantly by plant-specific chromomethylases (Bernstein et al., 2007, Bewick et al.,
400 2017, Henderson and Jacobsen, 2007). Further, it is to be noted that, spacer promoters in
401 animal models (e.g., frog species *Xenopus laevis*) significantly contribute to the
402 enhancement of rRNA gene transcription (De Winter and Moss, 1986). In contrast, spacer
403 promoters have minimal contribution, if any, to rRNA gene transcription, in plant species (e.g.
404 *Arabidopsis thaliana*) (Doelling et al., 1993). These findings indicate the evolution of
405 divergent rRNA gene regulation mechanisms in plants and animals.
406 The silent *NOR2* genes are hypermethylated in all cytosine contexts (CG, CHG, and
407 CHH) and exist in more condensed chromatin state than the active *NOR4* rRNA genes (Figs.
408 5-7) (Fultz et al., 2023, Mo et al., 2023). However, despite the striking similarities in rRNA
409 gene sequences between *NOR2* and *NOR4*, why rRNA genes on *NOR2* are selectively
410 hypermethylated and silenced? The question remains to be answered.
411
412 **Materials and Methods**
413 ***Plant material and growth***
414 *A. thaliana* ecotype Col-0 (stock no. CS22681), and mutants *met1-7* (stock no.
415 SALK_076522), *cmt2-3* (stock no. SALK_012874C), and *cmt3-11t* (stock no. SALK_148381),
416 were obtained from the Arabidopsis Biological Resource Center (ABRC; http://abrc.osu.edu).
417 *drm2-2b* (stock no. SAIL_70_E12) and $Col^{Sf\text{-}NOR4}$ (Chandrasekhara et al., 2016, Lee and
418 Amasino, 1995) were provided by Andrzej Wierzbicki and Scott Michaels, respectively, and
419 *ddm1-2* was provided by Eric Richards. Plants were grown in soil in a plant growth room
420 under a 16-h light/8-h dark photoperiod cycle with 50–55% humidity and temperature of 23–
421 25°C.
422
423 ***RNA isolation***
424 Four-week-old leaf tissue of individual plants was frozen in liquid nitrogen and ground into a
425 fine powder. RNeasy Plant Mini Kit (Qiagen) was used to extract total RNA from ground
426 powder. Total RNA was then treated with Turbo DNA-free kit (Invitrogen) to eliminate
427 contaminating DNA.

428 ***PCR and RT-PCR assays***

429 For PCR of genomic DNA to amplify all rRNA variants, PCR amplification was conducted
430 using 22-30 cycles (depending on the source of DNA) of 30 sec at 95°C, 30 sec at 55°C–
431 60°C, and 60 sec at 72°C. For RT–PCR, the reverse transcription reaction was performed
432 using 1 µg of total RNA using SuperScript III reverse transcriptase (Invitrogen). One
433 microliter (~100 ng) of reverse transcription product was then used for PCR amplification of
434 rRNA variable regions or actin gene control using 30 cycles of 30 sec at 94°C, 30 sec at
435 55°C, and 60 sec at 72°C. In all the PCR or RT-PCR reactions, primers 5'allvar and 3'allvar
436 were used to amplify rRNA variable regions (all four variant types). PCR and RT–PCR
437 products were resolved by electrophoresis on 2%–2.5% agarose gels in TBE buffer.
438 Sequences of primers used in this study are given in Figure S1.

439

440 ***Generation of DNA methylation heat maps***

441 Whole genome bisulfite sequencing data (GSE39901) published by Stroud et al.
442 (2013)(Stroud et al., 2013), was used to assess the methylation state of rDNA in various
443 methylation mutants. The sequencing data were analysed using Methylpy (Schultz et al.,
444 2015). The reads were mapped to a converted 45S rDNA reference sequence allowing a
445 single mismatch. The methylation state of all cytosines in CG, CHG, and CHH contexts was
446 then analyzed and represented as a fraction of methylated cytosines over the total cytosines
447 in each context. Replicates for a given genotype were merged into a single file.

448

449 ***DNA methylation map of the NOR2 and NOR4-adjacent regions***

450 DNA methylation profiles of the *NOR2* and *NOR4*-adjacent regions on *A. thaliana* Col-0
451 chromosomes 2 and 4 were compared using whole genome bisulfite sequencing data
452 published by Stroud et al. (2013) (GEO accession# GSM980986). In short, the
453 WT_rep2_CG.wig.gz, WT_rep2_CHG.wig.gz and WT_rep2_CHH.wig.gz data tracks
454 available in Wiggle format at https://www.ncbi.nlm.nih.gov/geo/ were used to display each
455 150 kb, centromere-proximal NOR-adjacent region in a local JBrowse instance with TAIR10
456 gene annotations and TE annotations of Buisine et al. (2008)

457

458 ***DNA isolation from leaf tissue and agarose gel pieces (gel elution).***

459 Genomic DNA (gDNA) was isolated from the leaf tissue of 4-week-old plants by using Illustra
460 Nucleon Phytopure extraction kit reagents (GE Healthcare). This gDNA was used for HindIII
461 CAPS assay (Figure 1C), PCR of rRNA variants (Figure 2, topmost panel), methylation
462 analysis of gDNA (Figure 5A left panel, Figure 5B, and Figure 6B, left panel). In some cases,
463 following gDNA PCR or digestion by methylation-sensitive enzymes, the products were

464 resolved on an agarose gel and the DNA fragments were gel-purified using QIAquick gel
465 extraction kit (Qiagen). This gel-purified DNA was subsequently used as a template for
466 downstream PCR amplification of rRNA variants (Figure 5B right panel, Figure 7C) or HindIII
467 CAPS assay (Figure 6B right panel). DNA from the EZ-Tn5 transposase-treated nuclei was
468 isolated using the cetyl trimethyl ammonium bromide (CTAB) method.
469
470 ***Nuclei isolation***
471 Nuclei were isolated using 10 g tissue from 3-week-old Col-0 plant seedlings as described
472 previously (Gaudino and Pikaard, 1997) with a few modifications. Briefly, 3-week-old plants
473 were harvested and washed in ice-cold water. Then the plants were submerged in cold
474 diethyl ether for 5 min and washed twice in ice-cold water. Homogenization of plant material
475 was performed in 100 mL of nuclei isolation buffer (1M sucrose, 50 mM Tris-HCl pH 7.2, 5
476 mM $MgCl_2$, 5 mM KCl, 10 mM 2-mercaptoethanol, 0.2 mM PMSF) with a motorized
477 homogenizer (Fisher Scientific Powergen 700). Homogenate was filtered through 1 layer of
478 Miracloth and 1 layer of nylon mesh (pore size of 50 μm). After centrifugation of the filtered
479 homogenate at 14,000 g for 15 min at 4°C the pellet was resuspended in 10 ml of nuclei
480 isolation buffer and prepared for loading into discontinuous Percoll gradient (15%, 30%, 45%,
481 and 60%) by adding one volume of "100% Percoll solution" (34.23 g sucrose, 5 mL 1 M Tris-
482 HCl pH 7.2, 0.5 mL 1 M $MgCl_2$, 0.5 mL 1 M KCl, 34 μL 2-mercaptoethanol, 100 μL 2 mM
483 PMSF and Percoll to 100 mL) to 19 volumes of nuclei. Gradients were centrifuged at 2,000
484 rpm for 10 min, then 8,000 rpm for 20 min. Nuclei were harvested from 30%/45% and
485 45%/60% boundaries and pooled. Nuclei were diluted with 5 volumes of nuclei isolation
486 buffer, mixed by inversion, and collected by centrifugation at 1,500 g for 10 min at 4°C. A
487 second wash of nuclei was performed with 25 volumes of nuclei isolation buffer. The final
488 wash was done with 50 mL of Nuclease digestion buffer (50 mM Tris-HCl, pH 8.0, 0.3 M
489 sucrose, 5 mM MgCl2, 1.5 mM NaCl, 0.1 mM CaCl2, 5 mM 2-mercaptoethanol). The
490 resulting pellet was resuspended in 2 mL of Nuclease digestion buffer.
491
492 ***Transposase-accessible chromatin assay***
493 The assay was carried out based on the methodology described by Buenrostro et al.
494 (Buenrostro et al., 2013). Oligos (5'-Ez-Tn5 and 3'-Ez-Tn5) were annealed by heating a
495 mixture of equal volumes of 100 mM oligos at 95 °C for 5 min, followed by turning the
496 heating off and incubating for 10 min. Transposition reactions were carried out using 2 μL of
497 purified nuclei, 20 μL of EZ-Tn5 transposase with varying amounts of the oligos 5'-Ez-Tn5
498 and 3'-Ez-Tn5, according to the manufacturer's instructions (Epicentre). Incubation was

499 performed at 37°C for 90 min. DNA was isolated using the cetyl trimethyl ammonium
500 bromide (CTAB) method. PCR1 and PCR2 were carried out as described above. The
501 sequences of primers and oligos used in this study are listed in Figure S1.
502
503
504 **Acknowledgements**
505 This work is supported by:
506 Birla Institute of Science and Technology (BITS) Pilani, Hyderabad campus through a
507 research grant to G.M. (BITS/GAU/ACRG/2019/H0576) and an Institute Fellowship to G.P.S.
508 Science and Engineering Research Board (SERB), Government of India through Ramanujan
509 Fellowship (SB-S2-RJN-062-2017) and CRG (CRG/2020/002855) research grants to GM,
510 and internship to N.V.P.
511 Department of Biotechnology through research grant (BT/PR38410/GET/119/310/2020) to
512 GM.
513 A.M. and R.E. were supported by funds to Craig S. Pikaard. as an investigator of the Howard
514 Hughes Medical Institute.
515 T.B. was supported by the ANR (ANR-17-CE20-0004), and by the Interdisciplinary Thematic
516 Institute IMCBio (ITI 2021-2028 program), including funds from IdEx University of Strasbourg
517 (ANR-10-IDEX-0002), SFRI-STRAT'US (ANR 20-SFRI-0012) and EUR IMCBio (ANR-17-
518 EURE-0023) in the framework of the French Investments for the Future Program.
519
520 We thank the members of the Pikaard lab and the Mohannath lab for their critique of the
521 manuscript.
522
523 **Competing interests**
524 The authors declare no competing interests.
525
526 **Author contributions**
527 A.M., R.E., N.V.P, G.P.S., and G.M. planned and designed the research; A.M., R.E., N.V.P.,
528 G.P.S., T.B., and G.M. performed the research; A.M., R.E., N.V.P, G.P.S., and G.M.
529 analysed the data; and A.M., R.E., N.V.P, G.P.S., and G.M. wrote the paper.
530
531 **Data availability**
532 For this article we analyzed the publicly available/published data, and the details are as
533 follows: The whole genome bisulfite sequencing data of *Arabidopsis thaliana* (WT and
534 mutants) were published by Stroud et al. (2013) (GEO accession# GSM980986). NOR-

535 adjacent methylation data are available at https://www.ncbi.nlm.nih.gov/geo/. The fully
536 assembled NOR sequences of *Arabidopsis thaliana* (strain Col-0) were published by Fultz et
537 al. (2023) and the sequences are available at GenBank as accessions OR453402
538 (https://ncbi.nlm.nih.gov/nuccore/OR453402) for *NOR2* and OR453401
539 (https://ncbi.nlm.nih.gov/nuccore/OR453401) for *NOR4*. Assembled whole genome
540 sequences of tomato (*Solanum lycopersicum*, cultivar Micro-Tom) have been published on a
541 preprint server Shirasawa and Ariizumi (2023) (https://doi.org/10.1101/2023.10.26.564283)
542 and the sequences are available at DDBJ (accession numbers AP028935–1 AP028946) and
543 KaTomicsDB (https://www.kazusa.or.jp/ tomato).
544

545 **Supplementary figure legends**

546 **Figure S1:** Primers/oligos used in this study.
547
548 **Figure S2:** The 45S rRNA gene reference sequence used to generate methylation heat
549 maps.
550
551 **Figure S3:** Occurrence of cytosines in the promoter regions of 45S rRNA genes.
552 Diagram depicting relative distribution of cytosines in CG, CHG, and CHH contexts in the
553 promoter regions of 45S rRNA genes in (A) Arabidopsis thaliana, and in (B) humans.
554
555 **Figure S4:** Centromere-proximal NOR2-adjoining region is hyper methylated compared to
556 the corresponding NOR4-adjoining region. Map of cytosine methylation in all sequence
557 contexts (CG, CHG and CHH) obtained for the wild-type plants (Col-0) using deep bisulfite
558 sequencing data. Methylation data for about 150 Kb region right next to the NORs on the
559 centromere-proximal side has been depicted. Height of the bars for each cytosine residue
560 indicates depth of the methylation at that residue. Annotated loci in the 150 Kb region are
561 shown above the methylation data.
562

563 **References**

564 ADEY, A., MORRISON, H. G., ASAN, XUN, X., KITZMAN, J. O., TURNER, E. H., STACKHOUSE, B.,
565 MACKENZIE, A. P., CARUCCIO, N. C., ZHANG, X. & SHENDURE, J. 2010. Rapid, low-input, low-
566 bias construction of shotgun fragment libraries by high-density in vitro transposition.
567 *Genome Biol,* 11**,** R119.
568 AHMED, A. 2009. Alternative mechanisms for tn5 transposition. *PLoS Genet,* 5**,** e1000619.

569 BACALINI, M. G., PACILLI, A., GIULIANI, C., PENZO, M., TRERÉ, D., PIRAZZINI, C., SALVIOLI, S.,
570 FRANCESCHI, C., MONTANARO, L. & GARAGNANI, P. 2014. The nucleolar size is associated to
571 the methylation status of ribosomal DNA in breast carcinomas. *BMC Cancer,* 14**,** 361.
572 BERNSTEIN, B. E., MEISSNER, A. & LANDER, E. S. 2007. The mammalian epigenome. *Cell,* 128**,** 669-81.
573 BEWICK, A. J., NIEDERHUTH, C. E., JI, L., ROHR, N. A., GRIFFIN, P. T., LEEBENS-MACK, J. & SCHMITZ, R.
574 J. 2017. The evolution of CHROMOMETHYLASES and gene body DNA methylation in plants.
575 *Genome Biol,* 18**,** 65.
576 BRZESKI, J. & JERZMANOWSKI, A. 2003. Deficient in DNA methylation 1 (DDM1) defines a novel
577 family of chromatin-remodeling factors. *J Biol Chem,* 278**,** 823-8.
578 BUENROSTRO, J. D., GIRESI, P. G., ZABA, L. C., CHANG, H. Y. & GREENLEAF, W. J. 2013. Transposition
579 of native chromatin for fast and sensitive epigenomic profiling of open chromatin, DNA-
580 binding proteins and nucleosome position. *Nat Methods,* 10**,** 1213-8.
581 BUISINE, N., QUESNEVILLE, H. & COLOT, V. 2008. Improved detection and annotation of transposable
582 elements in sequenced genomes using multiple reference sequence sets. *Genomics,* 91**,** 467-
583 75.
584 CHANDRASEKHARA, C., MOHANNATH, G., BLEVINS, T., PONTVIANNE, F. & PIKAARD, C. S. 2016.
585 Chromosome-specific NOR inactivation explains selective rRNA gene silencing and dosage
586 control in Arabidopsis. *Genes Dev,* 30**,** 177-90.
587 CHEN, Z. J. & PIKAARD, C. S. 1997. Epigenetic silencing of RNA polymerase I transcription: a role for
588 DNA methylation and histone modification in nucleolar dominance. *Genes Dev,* 11**,** 2124-36.
589 COKUS, S. J., FENG, S., ZHANG, X., CHEN, Z., MERRIMAN, B., HAUDENSCHILD, C. D., PRADHAN, S.,
590 NELSON, S. F., PELLEGRINI, M. & JACOBSEN, S. E. 2008. Shotgun bisulphite sequencing of the
591 Arabidopsis genome reveals DNA methylation patterning. *Nature,* 452**,** 215-9.
592 COPENHAVER, G. P., DOELLING, J. H., GENS, S. & PIKAARD, C. S. 1995. Use of RFLPs larger than 100
593 kbp to map the position and internal organization of the nucleolus organizer region on
594 chromosome 2 in Arabidopsis thaliana. *Plant J,* 7**,** 273-86.
595 COPENHAVER, G. P. & PIKAARD, C. S. 1996a. RFLP and physical mapping with an rDNA-specific
596 endonuclease reveals that nucleolus organizer regions of Arabidopsis thaliana adjoin the
597 telomeres on chromosomes 2 and 4. *Plant J,* 9**,** 259-72.
598 COPENHAVER, G. P. & PIKAARD, C. S. 1996b. Two-dimensional RFLP analyses reveal megabase-sized
599 clusters of rRNA gene variants in Arabidopsis thaliana, suggesting local spreading of variants
600 as the mode for gene homogenization during concerted evolution. *Plant J,* 9**,** 273-82.
601 COSTA-NUNES, P., PONTES, O., PREUSS, S. B. & PIKAARD, C. S. 2010. Extra views on RNA-dependent
602 DNA methylation and MBD6-dependent heterochromatin formation in nucleolar dominance.
603 *Nucleus,* 1**,** 254-9.
604 DE WINTER, R. F. & MOSS, T. 1986. Spacer promoters are essential for efficient enhancement of X.
605 laevis ribosomal transcription. *Cell,* 44**,** 313-8.
606 DOELLING, J. H., GAUDINO, R. J. & PIKAARD, C. S. 1993. Functional analysis of Arabidopsis thaliana
607 rRNA gene and spacer promoters in vivo and by transient expression. *Proc Natl Acad Sci U S*
608 *A,* 90**,** 7528-32.
609 DOELLING, J. H. & PIKAARD, C. S. 1995. The minimal ribosomal RNA gene promoter of Arabidopsis
610 thaliana includes a critical element at the transcription initiation site. *Plant J,* 8**,** 683-92.
611 DU, J., ZHONG, X., BERNATAVICHUTE, Y. V., STROUD, H., FENG, S., CARO, E., VASHISHT, A. A.,
612 TERRAGNI, J., CHIN, H. G., TU, A., HETZEL, J., WOHLSCHLEGEL, J. A., PRADHAN, S., PATEL, D. J.
613 & JACOBSEN, S. E. 2012. Dual binding of chromomethylase domains to H3K9me2-containing
614 nucleosomes directs DNA methylation in plants. *Cell,* 151**,** 167-80.
615 FULTZ, D., MCKINLAY, A., ENGANTI, R. & PIKAARD, C. S. 2023. Sequence and epigenetic landscapes of
616 active and silent nucleolus organizer regions in Arabidopsis. *Sci Adv,* 9**,** eadj4509.
617 GAUDINO, R. J. & PIKAARD, C. S. 1997. Cytokinin induction of RNA polymerase I transcription in
618 Arabidopsis thaliana. *J Biol Chem,* 272**,** 6799-804.

619 GERBI, S. A. 1986. The evolution of eukaryotic ribosomal DNA. *Biosystems,* 19**,** 247-58.
620 GHOSHAL, K., MAJUMDER, S., DATTA, J., MOTIWALA, T., BAI, S., SHARMA, S. M., FRANKEL, W. &
621 JACOB, S. T. 2004. Role of human ribosomal RNA (rRNA) promoter methylation and of
622 methyl-CpG-binding protein MBD2 in the suppression of rRNA gene expression. *J Biol Chem,*
623 279**,** 6783-93.
624 GORYSHIN, I. Y. & REZNIKOFF, W. S. 1998. Tn5 in vitro transposition. *J Biol Chem,* 273**,** 7367-74.
625 GRUMMT, I. 2013. The nucleolus—guardian of cellular homeostasis and genome integrity.
626 *Chromosoma,* 122**,** 487-97.
627 HANNAN, K. M., SANIJ, E., ROTHBLUM, L. I., HANNAN, R. D. & PEARSON, R. B. 2013. Dysregulation of
628 RNA polymerase I transcription during disease. *Biochim Biophys Acta,* 1829**,** 342-60.
629 HENDERSON, I. R. & JACOBSEN, S. E. 2007. Epigenetic inheritance in plants. *Nature,* 447**,** 418-24.
630 JEDDELOH, J. A., STOKES, T. L. & RICHARDS, E. J. 1999. Maintenance of genomic methylation requires
631 a SWI2/SNF2-like protein. *Nat Genet,* 22**,** 94-7.
632 KARAHAN, G., SAYAR, N., GOZUM, G., BOZKURT, B., KONU, O. & YULUG, I. G. 2015. Relative
633 expression of rRNA transcripts and 45S rDNA promoter methylation status are dysregulated
634 in tumors in comparison with matched-normal tissues in breast cancer. *Oncol Rep,* 33**,** 3131-
635 45.
636 LAW, J. A. & JACOBSEN, S. E. 2010. Establishing, maintaining and modifying DNA methylation
637 patterns in plants and animals. *Nat Rev Genet,* 11**,** 204-20.
638 LEE, I. & AMASINO, R. M. 1995. Effect of Vernalization, Photoperiod, and Light Quality on the
639 Flowering Phenotype of Arabidopsis Plants Containing the FRIGIDA Gene. *Plant Physiol,* 108**,**
640 157-162.
641 LEE, S. C., ADAMS, D. W., IPSARO, J. J., CAHN, J., LYNN, J., KIM, H. S., BERUBE, B., MAJOR, V.,
642 CALARCO, J. P., LEBLANC, C., BHATTACHARJEE, S., RAMU, U., GRIMANELLI, D., JACOB, Y.,
643 VOIGT, P., JOSHUA-TOR, L. & MARTIENSSEN, R. A. 2023. Chromatin remodeling of histone H3
644 variants by DDM1 underlies epigenetic inheritance of DNA methylation. *Cell,* 186**,** 4100-
645 4116.e15.
646 LEWIS, M. S. & PIKAARD, C. S. 2001. Restricted chromosomal silencing in nucleolar dominance. *Proc*
647 *Natl Acad Sci U S A,* 98**,** 14536-40.
648 LISTER, R., O'MALLEY, R. C., TONTI-FILIPPINI, J., GREGORY, B. D., BERRY, C. C., MILLAR, A. H. & ECKER,
649 J. R. 2008. Highly integrated single-base resolution maps of the epigenome in Arabidopsis.
650 *Cell,* 133**,** 523-36.
651 LONG, E. O. & DAWID, I. B. 1980. Repeated genes in eukaryotes. *Annu Rev Biochem,* 49**,** 727-64.
652 MATYÁŠEK, R., KALFUSOVÁ, R., KUDEROVÁ, A., ŘEHŮŘKOVÁ, K., SOCHOROVÁ, J. & KOVAŘÍK, A. 2024.
653 Transcriptional Silencing of 35S rDNA in Tragopogon porrifolius Correlates with Cytosine
654 Methylation in Sequence-Specific Manner. *Int J Mol Sci,* 25.
655 MO, W., SHU, Y., LIU, B., LONG, Y., LI, T., CAO, X., DENG, X. & ZHAI, J. 2023. Single-molecule targeted
656 accessibility and methylation sequencing of centromeres, telomeres and rDNAs in
657 Arabidopsis. *Nat Plants,* 9**,** 1439-1450.
658 MOHANNATH, G., PONTVIANNE, F. & PIKAARD, C. S. 2016. Selective nucleolus organizer inactivation
659 in Arabidopsis is a chromosome position-effect phenomenon. *Proc Natl Acad Sci U S A,* 113**,**
660 13426-13431.
661 MOSS, T., LANGLOIS, F., GAGNON-KUGLER, T. & STEFANOVSKY, V. 2007. A housekeeper with power
662 of attorney: the rRNA genes in ribosome biogenesis. *Cell Mol Life Sci,* 64**,** 29-49.
663 OSAKABE, A., JAMGE, B., AXELSSON, E., MONTGOMERY, S. A., AKIMCHEVA, S., KUEHN, A. L.,
664 PISUPATI, R., LORKOVIĆ, Z. J., YELAGANDULA, R., KAKUTANI, T. & BERGER, F. 2021. The
665 chromatin remodeler DDM1 prevents transposon mobility through deposition of histone
666 variant H2A.W. *Nat Cell Biol,* 23**,** 391-400.
667 PIKAARD, C. S., CHANDRASEKHARA, C., MCKINLAY, A., ENGANTI, R. & FULTZ, D. 2023. Reaching for
668 the off switch in nucleolar dominance. *Plant J,* 115**,** 1185-1192.

669 PONTVIANNE, F., ABOU-ELLAIL, M., DOUET, J., COMELLA, P., MATIA, I., CHANDRASEKHARA, C.,
670 DEBURES, A., BLEVINS, T., COOKE, R., MEDINA, F. J., TOURMENTE, S., PIKAARD, C. S. & SAEZ-
671 VASQUEZ, J. 2010. Nucleolin is required for DNA methylation state and the expression of
672 rRNA gene variants in Arabidopsis thaliana. *PLoS Genet,* 6**,** e1001225.
673 PONTVIANNE, F., BLEVINS, T., CHANDRASEKHARA, C., FENG, W., STROUD, H., JACOBSEN, S. E.,
674 MICHAELS, S. D. & PIKAARD, C. S. 2012. Histone methyltransferases regulating rRNA gene
675 dose and dosage control in Arabidopsis. *Genes Dev,* 26**,** 945-57.
676 PONTVIANNE, F., BLEVINS, T., CHANDRASEKHARA, C., MOZGOVA, I., HASSEL, C., PONTES, O. M.,
677 TUCKER, S., MOKROS, P., MUCHOVA, V., FAJKUS, J. & PIKAARD, C. S. 2013. Subnuclear
678 partitioning of rRNA genes between the nucleolus and nucleoplasm reflects alternative
679 epiallelic states. *Genes Dev,* 27**,** 1545-50.
680 PRIYADARSHINI, N., VENKATARAMA PUPPALA, N., PEROTH JAYAPRAKASH, J., KHANDELIA, P.,
681 SHARMA, V. & MOHANNATH, G. 2023. Ribosomal RNA gene downregulation in head and
682 neck squamous carcinoma cells correlates with rDNA promoter hypermethylation. *Gene***,**
683 147793.
684 RAVAL, A., SRIDHAR, K. J., PATEL, S., TURNBULL, B. B., GREENBERG, P. L. & MITCHELL, B. S. 2012.
685 Reduced rRNA expression and increased rDNA promoter methylation in CD34+ cells of
686 patients with myelodysplastic syndromes. *Blood,* 120**,** 4812-8.
687 RHEE, I., BACHMAN, K. E., PARK, B. H., JAIR, K. W., YEN, R. W., SCHUEBEL, K. E., CUI, H., FEINBERG, A.
688 P., LENGAUER, C., KINZLER, K. W., BAYLIN, S. B. & VOGELSTEIN, B. 2002. DNMT1 and
689 DNMT3b cooperate to silence genes in human cancer cells. *Nature,* 416**,** 552-6.
690 RYMEN, B., FERRAFIAT, L. & BLEVINS, T. 2020. Non-coding RNA polymerases that silence
691 transposable elements and reprogram gene expression in plants. *Transcription,* 11**,** 172-191.
692 SARADADEVI, G. P., PRIYADARSHINI, N., BERA, A. & MOHANNATH, G. 2020. Together we are on
693 together we are off -a conserved rule for ribosomal RNA (rRNA) gene regulation? *Journal of*
694 *Plant Biochemistry and Biotechnology,* 29**,** 743-753.
695 SASAKI, E., KAWAKATSU, T., ECKER, J. R. & NORDBORG, M. 2019. Common alleles of CMT2 and
696 NRPE1 are major determinants of CHH methylation variation in Arabidopsis thaliana. *PLoS*
697 *Genet,* 15**,** e1008492.
698 SCHULTZ, M. D., HE, Y., WHITAKER, J. W., HARIHARAN, M., MUKAMEL, E. A., LEUNG, D., RAJAGOPAL,
699 N., NERY, J. R., URICH, M. A., CHEN, H., LIN, S., LIN, Y., JUNG, I., SCHMITT, A. D., SELVARAJ, S.,
700 REN, B., SEJNOWSKI, T. J., WANG, W. & ECKER, J. R. 2015. Human body epigenome maps
701 reveal noncanonical DNA methylation variation. *Nature,* 523**,** 212-6.
702 SHIRASAWA, K. & ARIIZUMI, T. 2023. Near-complete genome assembly of tomato (Solanum
703 lycopersicum) cultivar Micro-Tom. *bioRxiv***,** 2023.10.26.564283.
704 STROUD, H., GREENBERG, M. V., FENG, S., BERNATAVICHUTE, Y. V. & JACOBSEN, S. E. 2013.
705 Comprehensive analysis of silencing mutants reveals complex regulation of the Arabidopsis
706 methylome. *Cell,* 152**,** 352-64.
707 TUROWSKI, T. W. & TOLLERVEY, D. 2015. Cotranscriptional events in eukaryotic ribosome synthesis.
708 *Wiley Interdiscip Rev RNA,* 6**,** 129-39.
709 VIKTOROVSKAYA, O. V. & SCHNEIDER, D. A. 2015. Functional divergence of eukaryotic RNA
710 polymerases: unique properties of RNA polymerase I suit its cellular role. *Gene,* 556**,** 19-26.
711 VONGS, A., KAKUTANI, T., MARTIENSSEN, R. A. & RICHARDS, E. J. 1993. Arabidopsis thaliana DNA
712 methylation mutants. *Science,* 260**,** 1926-8.
713 ZEMACH, A., KIM, M. Y., HSIEH, P. H., COLEMAN-DERR, D., ESHED-WILLIAMS, L., THAO, K., HARMER,
714 S. L. & ZILBERMAN, D. 2013. The Arabidopsis nucleosome remodeler DDM1 allows DNA
715 methyltransferases to access H1-containing heterochromatin. *Cell,* 153**,** 193-205.
716 ZHANG, X., YAZAKI, J., SUNDARESAN, A., COKUS, S., CHAN, S. W., CHEN, H., HENDERSON, I. R., SHINN,
717 P., PELLEGRINI, M., JACOBSEN, S. E. & ECKER, J. R. 2006. Genome-wide high-resolution
718 mapping and functional analysis of DNA methylation in arabidopsis. *Cell,* 126**,** 1189-201.

ZHOU, H., WANG, Y., LV, Q., ZHANG, J., WANG, Q., GAO, F., HOU, H., ZHANG, H., ZHANG, W. & LI, L. 2016. Overexpression of Ribosomal RNA in the Development of Human Cervical Cancer Is Associated with rDNA Promoter Hypomethylation. *PLoS One,* 11**,** e0163340.

ZILBERMAN, D., GEHRING, M., TRAN, R. K., BALLINGER, T. & HENIKOFF, S. 2007. Genome-wide analysis of Arabidopsis thaliana DNA methylation uncovers an interdependence between methylation and transcription. *Nat Genet,* 39**,** 61-9.

Figure Legends

Figure 1: Ribosomal RNA (rRNA) gene organization, subtype variation, localization, and their relative arrangement. (A) The diagram shows a generic tandem arrangement of 45S rRNA genes on a NOR. (B) The diagram shows the 3' ETS region of 45S rRNA genes that exhibit length and sequence polymorphisms among the rRNA variants. (C) The gel image shows HindIII CAPS assay of rRNA variants and the diagram at the bottom shows the position of HindIII restriction site relative to the binding sites of primers that amplify all four rRNA variants. (D) The diagram shows known locations of the rRNA variants on *NOR2* and *NOR4* in the Col-0 ecotype of *A. thaliana*.

Figure 2: Disruption of *NOR2* gene silencing to varying degrees in DNA methylation mutants. The gel images show DNA-PCR data for rRNA gene subtypes and RT-PCR expression data for rRNA gene subtypes and actin. The gel images were spliced to remove the second lane.

Figure 3: Methylation state of rDNA in CG, CHG, and CHH contexts. Whole genome bisulfite sequencing data from various DNA methylation mutants were analyzed using Methylpy, and the overall cytosine methylation state of rDNA is shown as heatmaps in all three cytosine contexts. The Y-axis represents a single rDNA unit starting with a promoter and ending with 3' ETS. Each line on the heatmap represents the methylation state of the cytosines in a given methylation context in 50 nucleotide bins. CG is shown in red, CHG in green, and CHH in blue. Grey indicates that no methylation sites were present in that bin for a given context.

TSS= Transcription Start Site.

Figure 4: Cytosines in the promoters of 45S rRNA genes occur mostly in CHH, distantly followed by CHG, and almost none in CG context.

755 (A) Relative distribution of cytosines among different cytosine contexts (CG, CHG, and CHH)
756 in the minimal rDNA promoter regions of different plant species. (B) For *A. thaliana* and
757 tomato, publicly available assembled NOR sequences were analyzed to quantify the number
758 of 45S rRNA gene repeats which show 100% conserved gene promoter sequence (-55 to
759 +6).
760 NA-Entire NOR sequences not available.
761
762 **Figure 5***: NOR2* genes are hypermethylated and *NOR4* genes are hypomethylated. (A) Gel
763 images on the left show resolution of HpaII- or buffer-treated Col-0 and *met1-7* DNA
764 samples, and the gel images on the right show PCR amplification of rRNA gene subtypes.
765 For these PCR reactions, gel-eluted DNA samples representing the HpaII-undigested (⩾ 20
766 kb) and the HpaII-digested (0.6-1.0 kb) fractions were used. (B) The gel images show rRNA
767 gene subtype PCR products obtained from McrBC-digested or no enzyme-treated Col-0
768 DNA.
769
770 **Figure 6**: Col-0 *NOR2* genes are hypermethylated and Sf-2 *NOR4* genes are
771 hypomethylated in the $Col^{Sf\text{-}NOR4}$ introgression line. (A) Diagram showing rRNA subtype
772 composition of the Arabidopsis introgression line called $Col^{Sf\text{-}NOR4}$ in which Sf-2 *NOR4* and
773 adjacent sequences were introgressed into the Col-0 genetic background. (B) The agarose
774 gel images on the left show resolution of HpaII- or buffer-treated $Col^{Sf\text{-}NOR4}$ gDNA samples,
775 and the gel images on the right show PCR amplification of rRNA variants with or without
776 HindIII digestion. For these PCR reactions, gel-eluted DNA samples representing the HpaII-
777 undigested (⩾ 20 kb) and the HpaII-digested (0.6-1.0 kb) fractions were used. (C) Summary
778 of results shown in (B). (D) The gel images show PCR amplification of rRNA variants
779 obtained from McrBC- or buffer-treated $Col^{Sf\text{-}NOR4}$ gDNA with or without HindIII digestion. (E)
780 Summary of results shown in (D).
781
782 **Figure 7**: *NOR2* genes exist in a more condensed chromatin than *NOR4* genes. (A) Tn5
783 Transposase-accessible chromatin assay (ATAC) was performed on nuclei isolated from
784 wild-type Col-0 plants. (B) DNA isolated from transposase-treated nuclei was used in PCR1
785 to amplify ~2.8kb rRNA gene promoter-proximal upstream regions involving the 3' ETS of
786 the preceding gene and IGS. (C) The PCR1-amplified 2.8 kb fragments were gel-eluted
787 followed by PCR2, products of which are visualized on a 2.8% agarose gel stained with
788 ethidium bromide. Amplification of VAR1 and VAR2 genes from 3' ETS variable region from
789 genomic DNA (gDNA) as a control is shown in the first lane. (D) The PCR1-amplified 2.8 kb
790 fragments were gel-eluted followed by PCR3, products of which are visualized on a 2.8%

791 agarose gel stained with ethidium bromide. Here, PCR3 involves amplification of all rRNA
792 variants. Amplification of all rRNA variants from 3' ETS variable region from genomic DNA
793 (gDNA) as a control is shown in the first lane.
794
795 **Figure 8**: Model depicting a role for CMT2-dependent CHH methylation in rRNA gene
796 silencing in Arabidopsis. In Wild-type, NOR2 rRNA genes are methylated in all cytosine
797 contexts. Loss of RdDM-dependent mCHH does not affect rRNA gene silencing at NOR2.
798 However, loss of CMT2-mediated mCHH results in disruption of NOR2 rRNA gene silencing
799 and likely alleviates chromatin condensation at these loci. Collectively, these findings
800 suggest that CMT2-mediated CHH methylation plays a critical role in rRNA gene silencing.
801

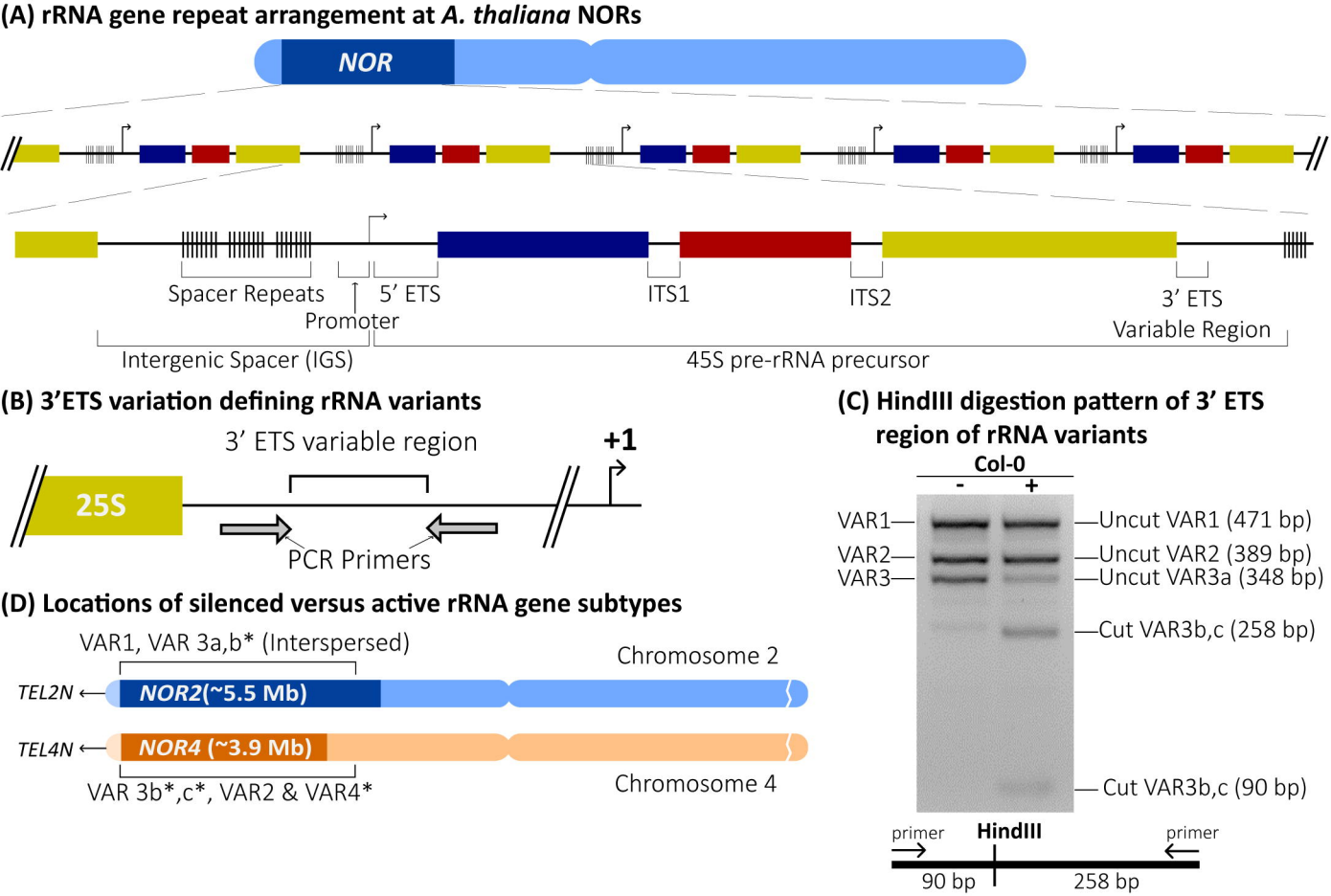

Figure 1. Ribosomal RNA (rRNA) gene organization, subtype variation, localization and their relative arrangement (A) The diagram shows a generic tandem arrangement of 45S rRNA genes on a NOR. (B) The diagram shows the 3' ETS region of 45S rRNA genes that exhibit length and sequence polymorphisms among the rRNA variants. (C) The gel image shows HindIII CAPS assay of rRNA variants and the diagram at the bottom shows the position of HindIII restriction site relative to the binding sites of primers that amplify all four rRNA variants. (D) The diagram shows known locations of the rRNA variants on *NOR2* and *NOR4* in the Col-0 ecotype of *A. thaliana.*

rRNA subtype expression in DNA methylation mutants

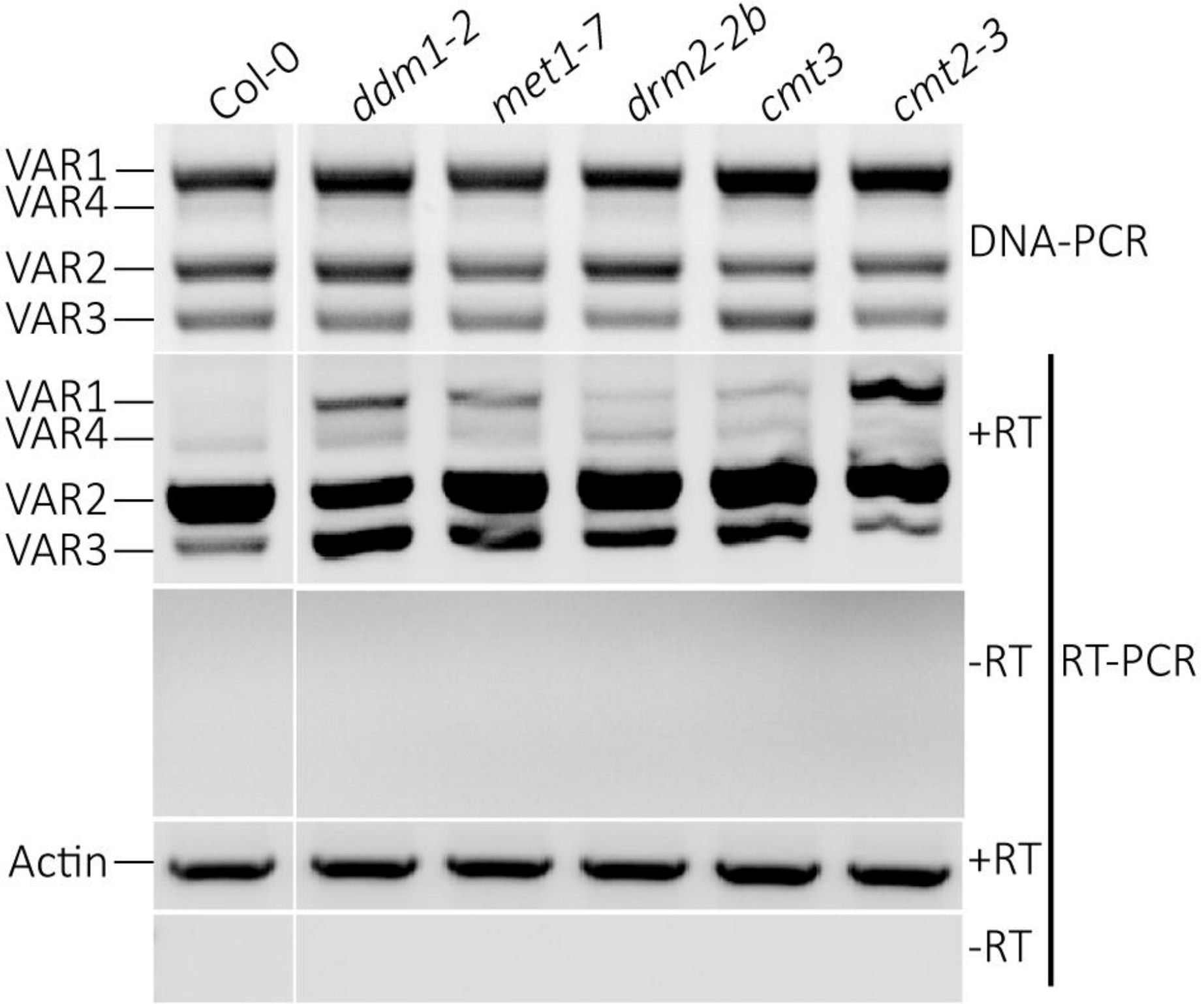

Figure 2. Disruption of *NOR2* gene silencing to varying degrees in DNA methylation mutants.

The gel images show DNA-PCR data for rRNA gene subtypes and RT-PCR expression data for rRNA gene subtypes and actin. The gel images were spliced to remove the second lane.

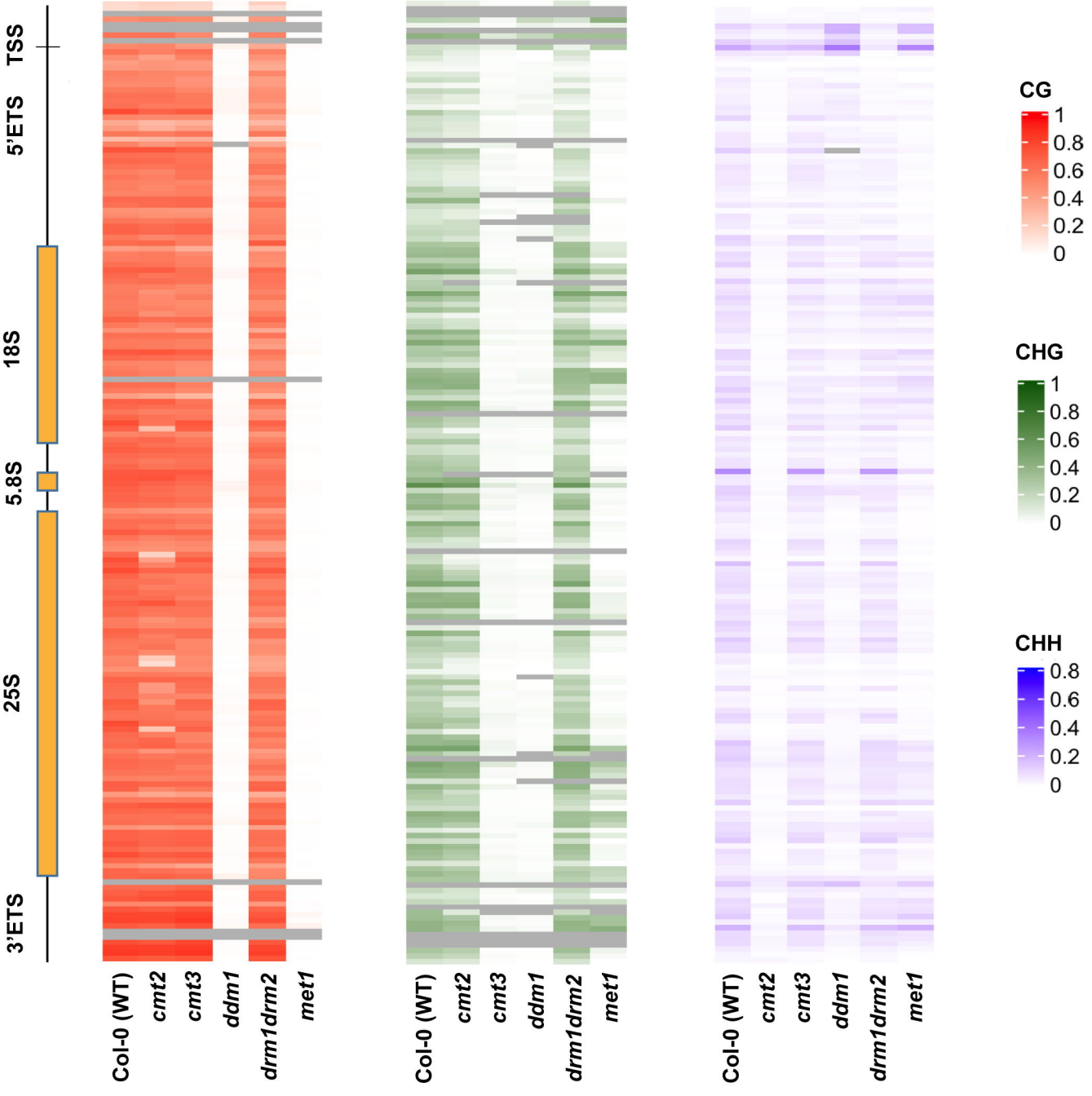

Figure 3: Methylation state of rDNA in CG, CHG, and CHH contexts. Whole genome bisulfite sequencing data from various DNA methylation mutants were analyzed using Methylpy, and the overall cytosine methylation state of rDNA is shown as heatmaps in all three cytosine contexts. The Y-axis represents a single rDNA unit starting with a promoter and ending with 3' ETS. Each line on the heatmap represents the methylation state of the cytosines in a given methylation context in 50 nucleotide bins. CG is shown in red, CHG in green, and CHH in blue. Grey indicates that no methylation sites were present in that bin for a given context. TSS= Transcription Start Site

(A)

45S rDNA gene promoter

	-55 … -20 … +1	Reference
A. thaliana	TCAGACATTTCAATGTCTGTTGGTGCCAAGAGGGAAAAGGGCTATTAAGCTATATAGGGGG	Doelling & Pikaard, 1995; Fultz et al., 2023
Tomato	CTGGAAAATCCATGTCTACTCCTGTCACATGGGCAAAACTTTTTTAAGCATATATAAGGGG	Doelling & Pikaard, 1995; Shirasawa & Ariizumi, 2023
Radish	GGAACAGAACAATGTCGACTTGGTGAAAGACTGAAAAAAAGCTTAAGTGTTATATAGGGGG	Doelling & Pikaard, 1995
Pea	AGGGAAAAAGGGACCCAGTTGCTGCTAAAGCAGGACATGCAAATCAAGCTTATATAGGGGG	Doelling & Pikaard, 1995
Cucumber	CGGAAATTTCATATGCAAGCCTGCCAGACCAAAAAAGTCCAAAATGTACTATATAGGGGG	Doelling & Pikaard, 1995
N. benthamiana	CTCTGACAAAGCATGTCTACTCCTGAAATTTGGGTTTTTTTTTTTAAGTATATATAAGGGG	https://solgenomics.net/

(B)

	Total C	CG	CHG	CHH	Number of 45S rRNA gene repeats with conserved gene promoter sequence	Reference
A. thaliana	8	0	2	6	Total: 859 (out of 894) (*NOR2*: 509/518, *NOR4*: 350/376)	Fultz et al., 2023
Tomato	12	0	2	10	*NOR2*: 1473/1500	Shirasawa & Ariizumi, 2023
Radish	6	1	2	3	NA	Doelling & Pikaard, 1995
Pea	10	0	3	7	NA	Doelling & Pikaard, 1995
Cucumber	12	1	2	9	NA	Doelling & Pikaard, 1995
N. benthamiana	8	0	2	6	NA	https://solgenomics.net/

Figure 4. Cytosines in the promoters of 45S rRNA genes occur mostly in CHH, distantly followed by CHG, and almost none in CG context. (A) Relative distribution of cytosines among different cytosine contexts (CG, CHG, and CHH) in the minimal rDNA promoter regions of different plant species. (B) For *A. thaliana* and tomato, publicly available assembled NOR sequences were analyzed to quantify the number of 45S rRNA gene repeats which show 100% conserved gene promoter sequence (-55 to +6).
NA-Entire NOR sequences not available.

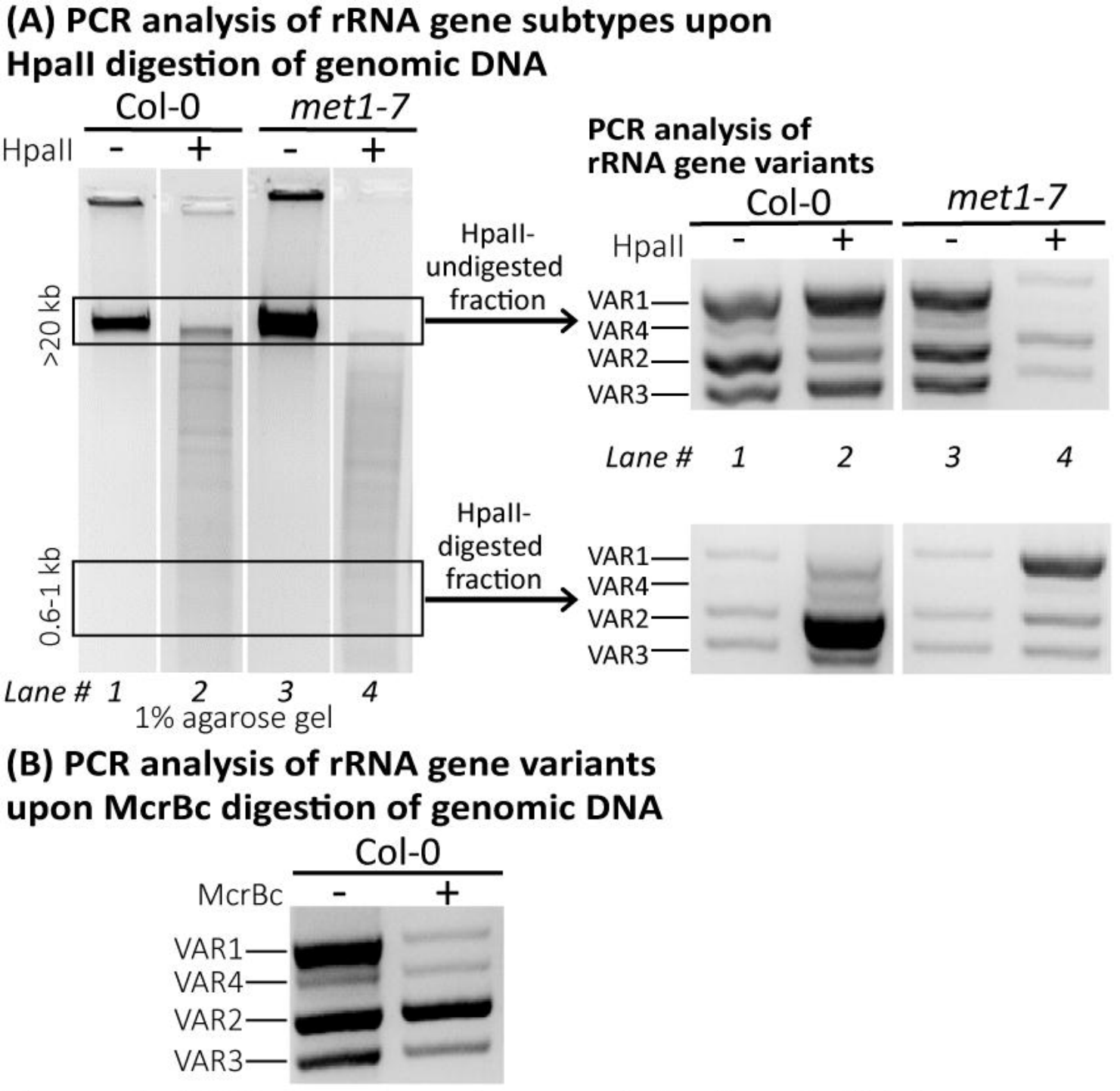

Figure 5. *NOR2* genes are hypermethylated and *NOR4* genes are hypomethylated.

(A) Gel images on the left show resolution of HpaII- or buffer-treated Col-0 and *met1-7* DNA samples and the gel images on the right show PCR amplification of rRNA gene subtypes. For these PCR reactions, gel-eluted DNA samples representing the HpaII-undigested (≥ 20 kb) and the HpaII-digested (0.6-1.0 kb) fractions were used. (B) The gel image shows rRNA gene subtype PCR products obtained from McrBc-digested or no enzyme-treated Col-0 DNA.

(A) Col$^{Sf\text{-}NOR4}$ line has Col-0 *NOR2* and Sf-2 *NOR4*

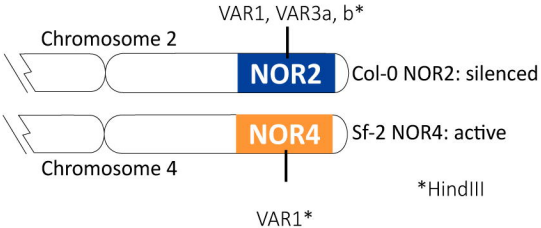

(B) HindIII CAPS analysis of rRNA gene subtypes amplified from gel-eluted fractions of HpaII-treated genomic DNA

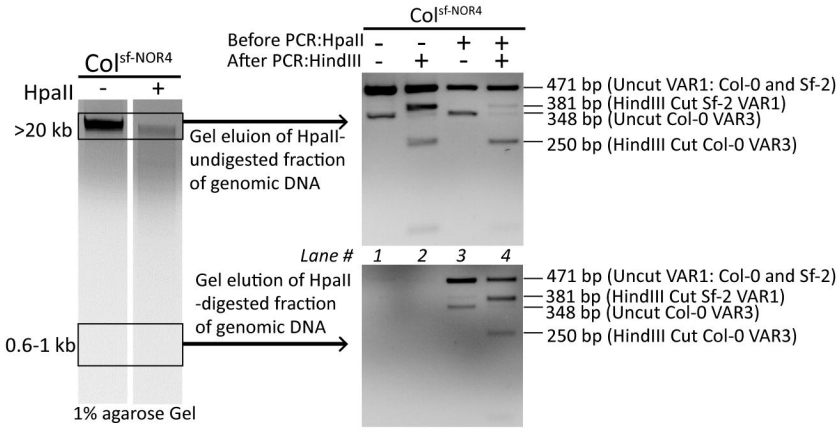

(C)

	rRNA variant composition of PCR amplicons	Position of HindIII in PCR amplicons	Relative DNA methylation status	Lane 1 (no enzyme control)	Lane 2 (HindIII after PCR)	Lane 3 (HpaII before PCR & No HindIII)	Lane 4 (HpaII before PCR & HindIII after PCR)
VAR1	Sf-2 VAR1 (471 bp)	F, HindIII, R; 90 bp, 381 bp	hypomethylated	uncut	cut	cut by HpaII	cut by HpaII & HindIII
VAR1	Colo-0 VAR1 (471 bp)	F, R	hypermethylated	uncut	uncut	uncut	uncut by HpaII or HindIII
VAR3	Col-0 VAR3a (348 bp)	F, R	hypermethylated	uncut	uncut	uncut	uncut by HpaII or HindIII
VAR3	Col-0 VAR3b (348 bp)	F, HindIII, R; 90 bp, 258 bp	hypermethylated	uncut	cut	uncut	uncut by HpaII but cut by HindIII

F-forward primer; R-reverse primer

(D) HindIII CAPS analysis of rRNA gene subtypes amplified from McrBc-treated genomic DNA

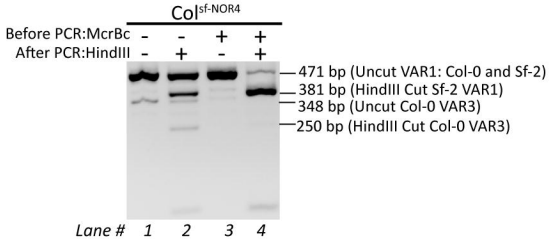

(E)

rRNA variant composition of PCR amplicons		Position of HindIII in PCR amplicons	Relative DNA methylation status	Lane 1 (no enzyme control)	Lane 2 (HindIII after PCR)	Lane 3 (McrBc before PCR & No HindIII)	Lane 4 (HpaII before PCR & HindIII after PCR)
VAR1	Sf-2 VAR1 (471 bp)	F HindIII R; 90 bp, 381 bp	hypomethylated	uncut	cut	uncut	uncut by McrBc & cut by HindIII
VAR1	Colo-0 VAR1 (471 bp)	F R	hypermethylated	uncut	uncut	cut by McrBc	cut by McrBc & uncut by HindIII
VAR3	Col-0 VAR3a (348 bp)	F R	hypermethylated	uncut	uncut	cut by McrBc	cut by McrBc & uncut by HindIII
VAR3	Col-0 VAR3b (348 bp)	F HindIII R; 90 bp, 258 bp	hypermethylated	uncut	cut	cut by McrBc	cut by McrBc & HindIII

F-forward primer; R-reverse primer

Figure 6. Col-0 *NOR2* genes are hypermethylated and Sf-2 *NOR4* genes are hypomethylated in the Col$^{sf\text{-}NOR4}$ introgression line. (A) Diagram showing rRNA subtype composition of the Arabidopsis introgression line called Col$^{sf\text{-}NOR4}$ in which Sf-2 *NOR4* and adjacent sequences were introgressed into the Col-0 genetic background. (B) The agarose gel images on the left show resolution of HpaII- or buffer-treated Col$^{sf\text{-}NOR4}$ gDNA samples, and the gel images on the right show PCR amplification of rRNA variants with or without HindIII digestion. For these PCR reactions, gel-eluted DNA samples representing the HpaII-undigested (≥ 20 kb) and the HpaII-digested (0.6-1.0 kb) fractions were used. (C) Summay of results shown in (B). (D) The Gel image shows PCR amplification of rRNA variants obtained from McrBc- or buffer-treated Col$^{sf\text{-}NOR4}$ gDNA with or without HindIII digestion. (E) Summary of results shown in (D).

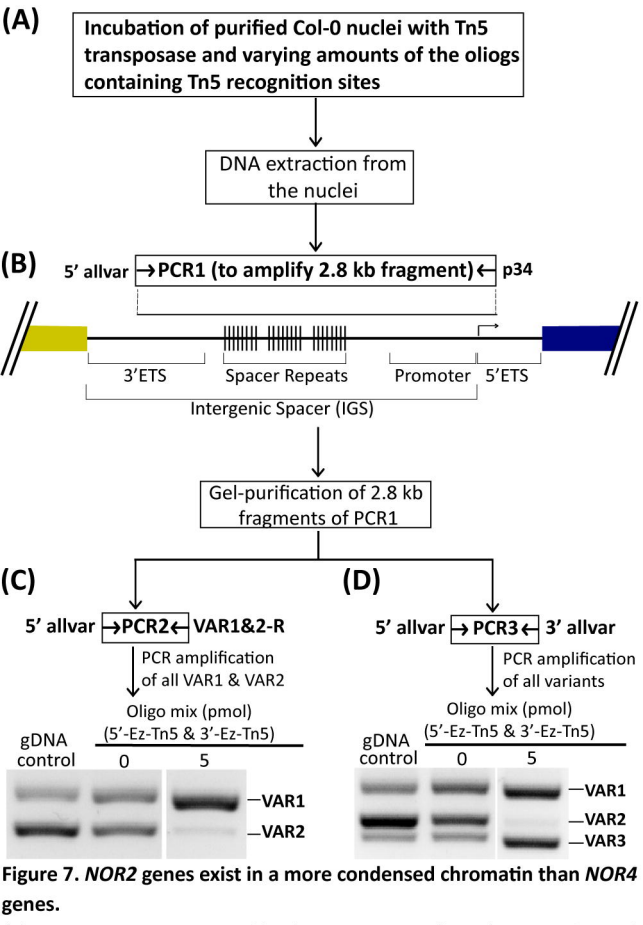

Figure 7. *NOR2* genes exist in a more condensed chromatin than *NOR4* genes.

(A) Tn5 Transposase-accessible chromatin assay (ATAC) was performed on nuclei isolated from wild-type Col-0 plants. (B) DNA isolated from the transposase-treated nuclei was used in PCR1 to amplify ~2.8 kb of rRNA gene promoter-proximal upstream regions involving the variable 3'ETS of the preceding gene and IGS. (C) The PCR1-amplified 2.8 kb fragments were gel-eluted followed by PCR2, products of which are visualized on a 1% agarose gel stained with ethidium bromide. Amplification of VAR1 and VAR2 genes from 3' ETS variable region from genomic DNA (gDNA) as a control is shown in the first lane. (D) The PCR1-amplified 2.8 kb gments were gel-eluted followed by PCR3, products of which are visualized on a 2.8% agarose gel stained with ethidium bromide. Here, PCR3 involves amplification of all rRNA variants. Amplification of all rRNA variants from 3' ETS variable region from genomic DNA (gDNA) as a control is shown in the first lane.

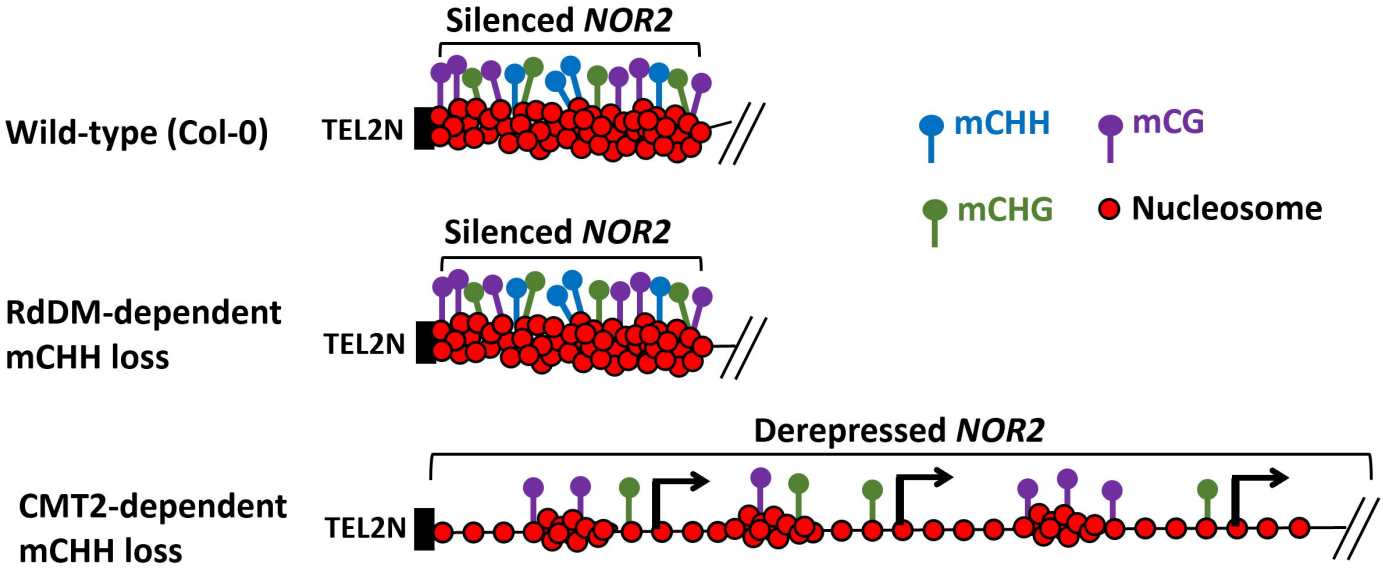

Figure 8. Model depicting a role for CMT2-dependent CHH methylation in rRNA gene silencing in Arabidopsis. In Wild-type, *NOR2* rRNA genes are methylated in all cytosine contexts. Loss of RdDM-dependent mCHH does not affect rRNA gene silencing at *NOR2.* However, loss of CMT2-mediated mCHH results in disruption of *NOR2* rRNA gene silencing and likely alleviates chromatin condensation at these loci. Collectively, these findings suggest that CMT2-mediated CHH methylation plays a critical role in rRNA gene silencing.